

Balanced Colorings and Bifurcations in Rivalry and Opinion Networks

Ian Stewart

Mathematics Institute

University of Warwick

Coventry CV4 7AL

United Kingdom

October 16, 2020

Abstract

Balanced colorings of networks classify robust synchrony patterns — those that are defined by subspaces that are flow-invariant for all admissible ODEs. In symmetric networks the obvious balanced colorings are orbit colorings, where colors correspond to orbits of a subgroup of the symmetry group. All other balanced colorings are said to be exotic. We analyze balanced colorings for two closely related types of network encountered in applications: trained Wilson networks, which occur in models of binocular rivalry, and opinion networks, which occur in models of decision making. We give two examples of exotic colorings which apply to both types of network, and prove that Wilson networks with at most two learned patterns have no exotic colorings. We discuss how exotic colorings affect the existence and stability of branches for bifurcations of the corresponding model ODEs.

1 Introduction

We work in the ‘coupled cell’ network formalism of [16, 20, 41], which should be consulted for precise definitions and proofs. Section 3 provides a short summary. Networks consist of *nodes* connected by *arrows* (directed edges), both of which are partitioned into *types*. Each node represents a dynamical system, and arrows indicate couplings between these systems. Identical types determine identical dynamics or couplings. It is sometimes convenient to interpret a node as an ‘internal arrow’ from that node to itself. Multiple arrows and self-loops are permitted; indeed, they are required to simplify the theory.

Robust patterns of synchrony in networks are classified by *balanced colorings* of the nodes. A coloring assigns a color to each node, and it is balanced if nodes of the same color have color-isomorphic input sets — that is, the same number of arrows of each type with tail nodes of a given color. To each coloring is associated a subspace of the state space, called a *synchrony subspace*, in which the coordinates of nodes of a given color

are all equal. This synchrony subspace is invariant for the dynamics of any ODE whose structure is compatible with the network architecture — that is, for all *admissible ODEs* — if and only if the coloring is balanced.

The existence of these universal flow-invariant subspaces has strong implications for bifurcations of admissible ODEs, because states lying in such a subspace have the synchrony pattern specified by the coloring, and can be found by restricting the ODE to the subspace. Such restrictions are precisely the admissible ODEs for the *quotient network*, obtained by identifying nodes with the same color and preserving the colored input structure. Sets of synchronous nodes are often called *clusters* [30], and the restricted ODE on the quotient network describes the dynamics of the clusters.

Synchrony for all admissible ODEs may seem a strong condition, but weaker forms of synchrony that persist under small perturbations of the ODE also correspond to balanced colorings. This has been proved for hyperbolic equilibria ([20, Theorem 7.6], [36, Theorem 6.1]), and for hyperbolic periodic states ([14, Theorem 6.1]) with a technical assumption on the network architecture: see [36, Appendix]. It is plausibly conjectured to be true for all hyperbolic periodic states [16, Section 10], and for more complex dynamic trajectories under some kind of assumption about persistence of the underlying attractor under small perturbations. A central issue in this case is to find a suitable definition of this type of persistence.

In networks with symmetry, every subgroup Σ of the symmetry group Γ defines a balanced coloring, where colors correspond to the orbits of Σ . We call such a coloring an *orbit coloring*. The synchrony space is then the fixed-point space of Σ . However, *exotic* balanced colorings that are not of this form can exist for some symmetric networks. This was pointed out in [13] for a 12-node bidirectional ring with \mathbb{D}_{12} symmetry and for certain 2-color lattice patterns. Other examples are discussed in [2, 3], and for planar square and hexagonal lattices in [35, 38, 39].

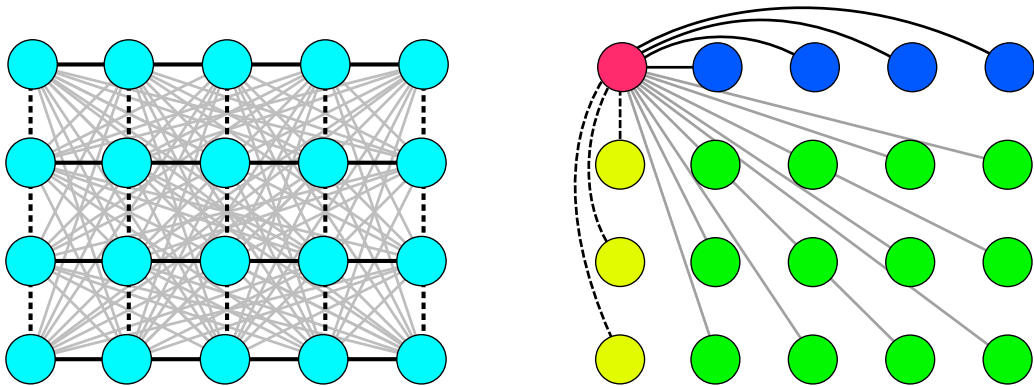


Figure 1: *Left*: Group network for $\mathbb{S}_4 \times \mathbb{S}_5$ acting on a 4×5 array. Only a representative set of connections shown. *Right*: The four arrow-types. Arrowheads not shown; only inputs to node $(1, 1)$ depicted. Colors of tail nodes and forms of edges indicate arrow-type: (a) red/internal arrow, (b) blue/solid, (c) yellow/dashed, (d) green/gray.

Here we study networks whose nodes form an $m \times n$ array. We assume the symmetry group is $\mathbb{S}_m \times \mathbb{S}_n$, where \mathbb{S}_m permutes the n rows and \mathbb{S}_n permutes the n columns, so all

nodes have the same type. Figure 1 (left) is a schematic illustration of the corresponding *group network* \mathcal{G}_{mn} in the sense of [2, Section 2]. There is one arrow for each ordered pair (i, j) of nodes, with head is i and tail j . The type of the arrow is given by the orbits of such pairs under the group action; arrows (i, i) correspond to the ‘internal arrow’ of node i and are represented by the node symbol, not an arrow as such. Figure 1 (right) is a schematic illustration of the inputs to node $(1, 1)$. There are four types of arrow:

- (a) Internal node arrow: circles.
- (b) Row arrows: solid black lines.
- (c) Column arrows: dashed black lines.
- (d) Diagonal arrows between nodes in neither the same row nor the same column: grey lines.

Admissible maps for a symmetric network are always equivariant under its symmetry group, but the converse is false in general, [2, Section 3.1]. In equivariant dynamical systems, every subspace that is flow-invariant for all equivariant ODEs is a fixed-point subspace [1, Theorem 4.1]. The possibility of exotic colorings can therefore be attributed to the difference between equivariant and admissible maps. The synchrony subspace of an exotic balanced coloring supports a pattern that is not an orbit coloring, hence not detected by the usual methods of equivariant dynamics.

The main point of this paper is the existence of exotic colorings in the networks \mathcal{G}_{36} and \mathcal{G}_{55} , shown below in Figures 3 and 4 respectively. (Similar methods can presumably extend this result to many larger values of m and n .) To complement these results, we also investigate networks arising in a model of binocular rivalry, showing that when these networks are trained on only one or two images, no exotic colorings exist. We postpone discussion to Section 6, after the models concerned have been introduced.

Finally, in Section 7 we discuss implications for bifurcations of admissible ODEs on the networks \mathcal{G}_{mn} . Exotic colorings indicate the presence of flow-invariant subspaces that are not detected by the usual method for finding bifurcating branches of symmetric dynamical systems, namely the Equivariant Branching Lemma. This proves the existence of certain symmetry-breaking patterns. The analogous phenomenon of synchrony-breaking patterns in networks can lead to exotic patterns, not predicted by their symmetries. Taking network constraints into account, as well as symmetry, gives a broader picture of the dynamics and bifurcations.

2 Networks Occurring in Applications

Our results apply to two closely related classes of symmetric networks occurring in applications. Both are variations on networks proposed by Wilson [45, 46, 47] to model interocular grouping, and more generally, high-level decision-making in the brain, and are called *Wilson networks*. An *untrained* Wilson network is a rectangular $m \times n$ array of identical nodes whose columns are all-to-all connected by identical inhibitory arrows. The symmetry group of this network is not $\mathbb{S}_m \times \mathbb{S}_n$, but the larger wreath product $\mathbb{S}_m \wr \mathbb{S}_n$ (permute the nodes in each column in any manner, and permute the columns setwise). Figure 2 shows (schematically) an untrained 5×8 Wilson network. For clarity, the dotted lines indicate sets of nodes — the columns — with identical all-to-all coupling.

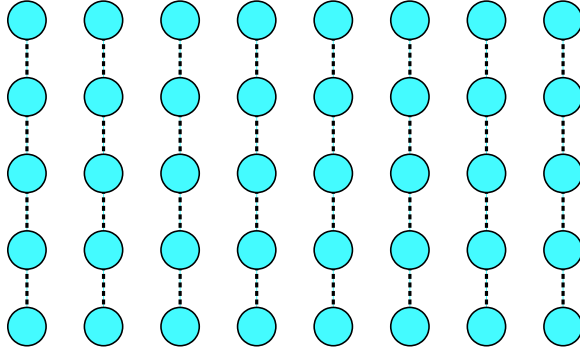


Figure 2: Untrained 5×8 Wilson network. Dotted lines indicate sets of nodes with identical all-to-all coupling. Columns are decoupled from each other.

2.1 Binocular Rivalry

The discovery of (binocular) rivalry is credited to Giambattista della Porta [31] in 1593. He placed two books so that each eye saw only one, and stated that he was able to read from either book at will by moving the ‘visual virtue’ (attention) from one eye to the other. Closely related but distinct phenomena are visual illusions, where a single image can be perceived in more than one way; the classic example is the Necker cube of 1832, Necker [28], which alternates between two apparent orientations. Numerous authors have modeled rivalry and illusions using a network with two nodes, representing the two percepts [7, 8, 22, 24, 25, 26, 27, 29, 32].

Modern experiments on rivalry show a different image to each eye and ask the subject to report what they perceive. In simple cases, these percepts alternate between those two images. In some studies, however, some subjects perceive not only the original two images, but images that combine aspects of those images in new ways [23, 33, 42, 43]. The occurrence of these *derived images* can be modelled using trained Wilson networks [9, 10, 11], also called rivalry networks. Experimental evidence supporting such models has been obtained in [21], which reports data on the 4-location experiment proposed in [43], obtaining results consistent with those predicted by a trained Wilson network model.

The model for a given pair of images begins with an untrained Wilson network. Each column represents an *attribute* of the image, such as the orientation or color of some feature. The nodes in a given column represent *levels* of that attribute, such as specific orientations or colors. The initial Wilson network is *trained* by adding excitatory arrows representing the *learned patterns* shown to the two eyes. A learned pattern is represented by a choice of one node from each column — the appropriate level of that attribute — connected all-to-all by identical excitatory arrows.

In standard model ODEs, the state of each node i is defined by two variables $(x_i^A, x_i^H) \in \mathbb{R}^2$. The first is an *activity* variable, the second a *fatigue* variable. Derived patterns emerge from the dynamics of an admissible ODE for the trained Wilson network. A balanced coloring of a Wilson network defines a *fusion state* in which the percept is ambiguous. If the fusion state becomes unstable, symmetry-breaking states can bifurcate. Such bifurcations are usually analysed using equivariant (symmetric) bifurcation theory. In the models under discussion, the relevant bifurcating branches consist of os-

cillatory states, created through an equivariant version of Hopf bifurcation. The main existence theorem here is the Equivariant Hopf Theorem [19, Chapter XVI Theorem 4.1], which guarantees the existence of branches with certain spatiotemporal symmetries — namely, \mathbb{C} -axial subgroups, which are those having 2-dimensional fixed-point spaces in a Liapunov-Schmidt reduction. Spatiotemporal symmetries describe patterns of synchrony and phase relations between nodes.

The interpretation of an oscillatory state associates the perceived image with the node or nodes whose activity variables are largest among all nodes. Changes in the ordering of activity levels indicate transitions between different percepts. However, the relation of symmetry to the network structure is subtle. In particular, exotic colorings predict behavior in such models that is not deducible from symmetries alone. So, potentially, exotic colorings can lead to branches with new types of spatiotemporal symmetry.

The main results of this paper for trained Wilson networks are:

- Every balanced coloring is an orbit coloring for the automorphism group of the resulting network when the network has been trained on 0, 1, or 2 learned patterns.
- The automorphism group concerned depends on the attribute levels of the images used to train the network.
- There exist exotic colorings when the network has been trained on 3 or more learned patterns.

Thus there can exist spatiotemporal patterns — in particular, synchrony patterns of oscillatory states and associated phase patterns — that are not predicted by the Equivariant Hopf Theorem. These patterns have not yet been investigated in any detail.

2.2 Decision Making

The notion of decision making is very broad. Virtually any collective system of active agents must make decisions. The agents can, for instance, be humans, birds in a flock, fish in a school, bees, bacteria, neurons, or autonomous robots. As preliminary step, agents form ‘opinions’ about a set of possible options; that is, preferences that affect the system’s behavior. These opinions collectively determine the eventual decision at system level. Examples of decision making systems include:

- Social and economic decisions by humans based on different types of electoral and information-sharing systems.
- Hunting strategies in past and present hunter-gatherer communities.
- Bee colonies collectively deciding on a new nest site.
- Animal groups collectively deciding when, and in which direction, to move — for example when approaching two possible food sources.
- Neurons in lower brain areas integrating sensory inputs to perform perceptual and motor behavior decision making.

- Neurons in higher brain areas integrating sensorimotor information to make higher-level decisions.
- Bacteria and other social microorganisms collectively deciding — for instance, by quorum sensing — how and when to undergo phenotypic differentiation in response to environmental signals.
- Swarms of autonomous robots settling on a collective strategy to accomplish some task.

The same mathematical models often apply to a variety of such real-world decision-making systems.

Here we focus on networks very similar to Wilson networks that have been introduced into models of decision making [12]. Again the nodes of the network form an $m \times n$ array, but now the columns represent options, the rows represent agents, and the state of a node represents the agent’s opinion about that option. Connections between nodes are of three types: distinct nodes in the same row, distinct nodes in the same column, and all other pairs of distinct nodes. The network has $\mathbb{S}_m \times \mathbb{S}_n$ symmetry where \mathbb{S}_m permutes the m rows and \mathbb{S}_n permutes the n columns.

The analysis of [12] focuses on steady-state symmetry-breaking bifurcation from a fully symmetric equilibrium, using the Equivariant Branching Lemma [5] (see also [15, Lemma 1.3.1] or [19, Chapter XIII Theorem 3.3]). This result states that, subject to certain genericity conditions, branches exist for all *axial* subgroups of the symmetry group — those with 1-dimensional fixed-point spaces. Classifying the axial subgroups therefore leads to a list of branches breaking symmetry in various ways. In this application the corresponding orbit colorings classify patterns of equal opinions about various options for various agents. These patterns govern agreements (consensus) and disagreements (dissensus) among the agents.

The states obtained using the Equivariant Branching Lemma need not exhaust the possible bifurcating branches, even for equivariant dynamical systems, but they provide useful information on symmetry-breaking states that are guaranteed to occur. In networks, the difference between equivariant and admissible ODEs can create branches that do not occur in general equivariant systems. In particular, exotic balanced colorings predict new branches that do not appear in any classification by isotropy subgroups.

The main result of this paper for opinion networks is:

- The examples of exotic colorings for trained Wilson networks can also be interpreted as exotic colorings for opinion networks.

3 Balanced Colorings and Automorphisms

We begin by recalling some basic concepts of the ‘coupled cell’ network formalism [20, 41].

Definition 3.1. A *network diagram* is a labelled directed graph that has four ingredients:

- (1) A finite set of *nodes* (or *cells*) $\mathcal{C} = \{1, 2, \dots, n\}$.

- (2) A *node symbol* assigned to each node. Nodes with the same symbol are said to be *identical*.
- (3) A finite set \mathcal{A} of *edges* or *arrows*. Each arrow e points from its *tail node* $\mathcal{T}(e)$ to its *head node* $\mathcal{H}(e)$.
- (4) An *arrow symbol* assigned to each arrow. Arrows with the same symbol are said to be *identical*.

The formal theory of networks goes on to define a class of *admissible maps* and associated *admissible ODEs* associated with the network. Essentially, these are the maps or ODEs that respect the network structure.

The *automorphism group* $\text{aut}(\mathcal{G})$ of a network \mathcal{G} consists of all permutations of the nodes \mathcal{C} that preserve the number and type of arrows between each pair of nodes.

The *input set* $I(c)$ consists of all input arrows to node c . An *input isomorphism* $\beta : I(c) \rightarrow I(d)$ is bijection that preserves arrow-type.

A *coloring* of \mathcal{G} is a partition of \mathcal{C} , or equivalently a map $K : \mathcal{C} \rightarrow \mathcal{K}$ where \mathcal{K} is a set of colors. A coloring is *balanced* if, whenever nodes c, d have the same color, there is an input isomorphism $\beta : I(c) \rightarrow I(d)$ such that $\mathcal{T}(e)$ and $\mathcal{T}(\beta(e))$ have the same color for all arrows $e \in \mathcal{A}$. As already remarked, a coloring is balanced if and only if it defines a synchrony subspace that is flow-invariant for all admissible ODEs, and the dynamics of the resulting clusters is given by the restricted admissible ODE on the *quotient network* whose nodes represent the clusters.

A subgroup $\Sigma \subseteq \text{aut}(\mathcal{G})$ defines a coloring K^Σ , where colors are determined by Σ -orbits on \mathcal{C} . That is, nodes have the same color if and only if they are in the same Σ -orbit. We call this the *orbit coloring* for Σ .

Proposition 3.2. *Every orbit coloring is balanced.*

Proof. This is [1, Proposition 3.3], stated using different terminology. In that paper, ‘orbit coloring’ is replaced by ‘fixed-point coloring’. \square

The *isotropy subgroup* Σ^K of a coloring K is the subgroup of $\text{aut}(\mathcal{G})$ that leaves every set of K setwise invariant, where K is considered as a partition of \mathcal{C} .

The next proposition is simple but useful:

Proposition 3.3. *A coloring is an orbit coloring if and only if it is the same (up to choice of colors) as the orbit coloring for K^Σ , where Σ is its isotropy subgroup.*

Proof. If $K = K^\Sigma$ then K is an orbit coloring. Conversely, let K be the orbit coloring for a subgroup Ω . Then $\Omega \subseteq \Sigma$ so $\text{Fix}(\Sigma) \subseteq \text{Fix}(\Omega)$. Let c, d be in the same Σ -orbit. Since Σ fixes the colors, c and d have the same color. Therefore $\text{Fix}(\Sigma) = \text{Fix}(\Omega)$ and $K^\Sigma = K$. \square

The next result is useful because some of the applications we discuss use networks like \mathcal{G}_{mn} but with arrows of type (d) deleted.

Lemma 3.4. *A coloring K is balanced for \mathcal{G}_{mn} provided it is balanced when type (d) arrows are deleted and type (a) ‘arrows’ are ignored.*

Proof. By [34, Lemma 5.4] a coloring is balanced if and only if it is balanced for each type of arrow separately — that is, in the network where arrows of all other types are deleted. This follows by counting arrows with tail node of a given color, and noting that input isomorphisms preserve arrow-type. If an input isomorphism also preserve colors of tail nodes, it must preserve colors of tail nodes of arrows of each type separately.

For \mathcal{G}_{mn} , balance for type (a) internal arrows is trivial. Moreover, balance for type (d) arrows is a consequence of balance for both types (b) and (c), because there is a unique arrow for each pair (i, j) and it therefore has a unique type. \square

4 Existence of Exotic Colorings

We now give two examples of exotic balanced colorings in networks \mathcal{G}_{mn} when $(m, n) = (3, 6)$ and $(5, 5)$.

4.1 The Network \mathcal{G}_{36}

The first example is \mathcal{G}_{36} , Figure 3, where we omit type (d) arrows and show types (b) and (c) schematically. By Lemma 3.4 the omission of type (d) arrows does not affect balance.

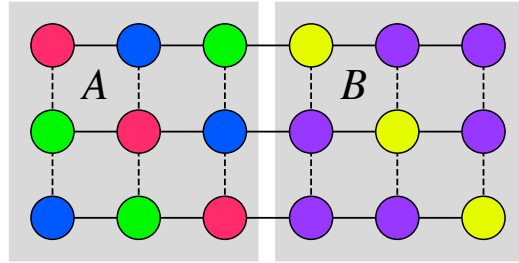


Figure 3: Exotic balanced coloring of \mathcal{G}_{36} . Type (d) arrows omitted, without loss of generality.

Theorem 4.1. *The coloring in Figure 3 is balanced, but is not an orbit coloring.*

Proof. It is easy to prove that the pattern in Figure 3 is balanced. Each row contains the same colors with the same multiplicities, so it is balanced with respect to the type (b) connections. Columns either have the same colors with the same multiplicities, or a disjoint set of colors. So the pattern is balanced with respect to the type (c) connections. Therefore it is balanced.

We claim it is not an orbit coloring. Suppose for a contradiction that it is the orbit coloring of a subgroup $\Sigma \subseteq \mathbb{S}_3 \times \mathbb{S}_6$. Because the colors in regions A and B are disjoint, we must have

$$\Sigma \subseteq \mathbb{S}_3^R \times \mathbb{S}_3^A \times \mathbb{S}_3^B$$

where \mathbb{S}_3^R permutes the rows, \mathbb{S}_3^A permutes columns 1, 2, 3 and \mathbb{S}_3^B permutes columns 4, 5, 6. We identify these groups with the same group \mathbb{S}_3 and use R, A, B to indicate

which direct factor is intended. We ask when an element $(\alpha, \beta, \gamma) \in \mathbb{S}_3^R \times \mathbb{S}_3^A \times \mathbb{S}_3^B$ fixes the pattern. This gives its isotropy subgroup Σ . Then we show that the pattern is not given by the orbits of Σ .

Regions A and B in the figure (columns 1–3 and 4–6) have disjoint sets of colors. The isotropy subgroup Σ must preserve these colors, hence it must preserve regions A and B . Therefore Σ is the intersection of the isotropy subgroups Σ^A and Σ^B of the patterns in regions A and B . The isotropy group Σ^A clearly consists of all elements of the form

$$(\alpha, \alpha, \gamma) \quad \alpha \in \mathbb{Z}_3, \gamma \in \mathbb{S}_3$$

The isotropy group Σ^B clearly consists of all elements of the form

$$(\alpha, \beta, \alpha) \quad \alpha \in \mathbb{S}_3, \beta \in \mathbb{S}_3$$

(This has two orbits: the set of nodes in positions (i, i) ($1 \leq i \leq 3$) and the set of nodes in positions (i, j) ($1 \leq i \neq j \leq 3$). This is the 2-color pattern in region B .) Their intersection therefore consists of all elements of the form

$$(\alpha, \alpha, \alpha) \quad \alpha \in \mathbb{Z}_3$$

This group has order 3. It has six orbits, not five, so Lemma 3.4 implies that Figure 3 is not an orbit coloring. In fact, the orbit coloring for this group splits the six purple nodes in region B into two sets of three, with different colors, such that the same color occurs along each broken diagonal. \square

4.2 The Network \mathcal{G}_{55}

The example in the previous section involves two disjoint ‘blocks’ of colors in regions A and B . By passing to more learned patterns — five, to be precise — we can find an example with one block. We use a coloring of \mathcal{G}_{55} based on a Latin square to give an example of an exotic balanced coloring. Again we omit type (d) arrows and show types (b) and (c) schematically, appealing to Lemma 3.4.

Remark 4.2. The classification of 3×3 and 4×4 Latin squares [44] shows that no analogous examples exists with 3 or 4 learned patterns.

Theorem 4.3. *The coloring in Figure 4 is balanced, but is not an orbit coloring.*

Proof. This coloring is balanced because every node receives exactly one type (b) connection and one type (c) connection from a node of any different color.

To prove that this coloring is not an orbit coloring, observe that the subgroup that fixes the black pattern is clearly the diagonal subgroup

$$\Delta = \{(\sigma, \sigma) : \sigma \in \mathbb{S}_5\} \subseteq \mathbb{S}_5 \times \mathbb{S}_5$$

For $\sigma \in \mathbb{S}_5$ define the permutation matrix P_σ by

$$(P_\sigma)_{ij} = \begin{cases} 1 & \text{if } j = \sigma(i) \\ 0 & \text{if } j \neq \sigma(i) \end{cases}$$

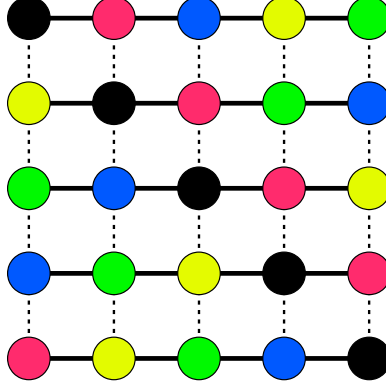


Figure 4: Exotic balanced coloring of \mathcal{G}_{55} . Type (d) arrows omitted, without loss of generality.

Let M be a 5×5 matrix. Then $P_\sigma M$ permutes the rows of M , sending row i to row $\sigma^{-1}(i)$. Similarly MP_σ permutes the columns of M , sending column j to column $\sigma(j)$. Thus an element $(\sigma, \sigma) \in \Delta$ can be considered as acting on the space of 5×5 matrices by conjugation:

$$M \mapsto P_\sigma M P_\sigma^{-1}$$

This permutes both rows and columns simultaneously, via the same permutation.

Define five matrices M_j corresponding to the positions of nodes of a given color:

$$M_1 = \begin{bmatrix} 1 & 0 & 0 & 0 & 0 \\ 0 & 1 & 0 & 0 & 0 \\ 0 & 0 & 1 & 0 & 0 \\ 0 & 0 & 0 & 1 & 0 \\ 0 & 0 & 0 & 0 & 1 \end{bmatrix} \quad M_2 = \begin{bmatrix} 0 & 1 & 0 & 0 & 0 \\ 0 & 0 & 1 & 0 & 0 \\ 0 & 0 & 0 & 1 & 0 \\ 0 & 0 & 0 & 0 & 1 \\ 1 & 0 & 0 & 0 & 0 \end{bmatrix} \quad M_3 = \begin{bmatrix} 0 & 0 & 1 & 0 & 0 \\ 0 & 0 & 0 & 0 & 1 \\ 0 & 1 & 0 & 0 & 0 \\ 1 & 0 & 0 & 0 & 0 \\ 0 & 0 & 0 & 1 & 0 \end{bmatrix}$$

$$M_4 = \begin{bmatrix} 0 & 0 & 0 & 1 & 0 \\ 1 & 0 & 0 & 0 & 0 \\ 0 & 0 & 0 & 0 & 1 \\ 0 & 0 & 1 & 0 & 0 \\ 0 & 1 & 0 & 0 & 0 \end{bmatrix} \quad M_5 = \begin{bmatrix} 0 & 0 & 0 & 0 & 1 \\ 0 & 0 & 0 & 1 & 0 \\ 1 & 0 & 0 & 0 & 0 \\ 0 & 1 & 0 & 0 & 0 \\ 0 & 0 & 1 & 0 & 0 \end{bmatrix}$$

We already know that the permutations (σ, τ) that fix the black nodes are those in Δ . So $(\sigma, \sigma) \in \Delta$ fixes all M_j (which is equivalent to fixing the coloring) if and only if

$$P_\sigma M_j P_\sigma^{-1} = M_j \quad 2 \leq j \leq 5$$

or equivalently

$$M_j P_\sigma = P_\sigma M_j \quad 2 \leq j \leq 5$$

Solving these equations using Mathematica, we find that

$$P_\sigma = \begin{bmatrix} a & b & b & b & b \\ b & a & b & b & b \\ b & b & a & b & b \\ b & b & b & a & b \\ b & b & b & b & a \end{bmatrix}$$

for $a, b \in \mathbb{R}$. This is a permutation matrix if and only if $a = 1, b = 0$, so the isotropy subgroup of the coloring is the identity. However, the fixed-point subspace of the identity contains all colorings, so the pattern in Figure 4 is not an orbit coloring. \square

5 Decision Making

Networks \mathcal{G}_{mn} occur in models of decision making [12]. We summarize the salient features. The model assumes that a group of m equal agents is trying to decide among a set of n options, initially assumed to be of equal value to all agents. This case is mathematically tractable because of its symmetry, and it is also important for examining more complex real-world settings. The equality assumptions are formalized as symmetries. Equation (2.11) of [12] defines a specific class of admissible ODEs, which is an equivariant version of a more general model [4]. The authors use the Equivariant Branching Lemma to prove the existence of various symmetry-breaking equilibria.

5.1 Exotic Colorings of Opinion Networks

We now discuss the difference between admissible maps for the network \mathcal{G}_{mn} and equivariant maps for $\mathbb{S}_m \times \mathbb{S}_n$. Recall from [20, 41] that the *vertex group* $B(i, i)$ at a node i of a network is the group of all input automorphisms on the set $I(i)$ of all input arrows of node i .

The proof of [1, Theorem 4.4] can easily be adapted to show that for a symmetric network, admissible maps are the same as equivariant maps if and only if:

- (a) The network is all-to-all connected.
- (b) Every vertex symmetry extends to an element of the symmetry group.

When the network is \mathcal{G}_{45} , for example, Figure 1 (right) shows that the vertex group of any node $c = (i, j)$ of \mathcal{G}_{mn} is

$$B(c, c) = \mathbb{S}_4 \times \mathbb{S}_3 \times \mathbb{S}_{12}$$

Condition (a) holds in this case, but

$$|B(c, c)| = 4! 3! 16! = 3012881743872000 \quad |\mathbb{S}_4 \times \mathbb{S}_5| = 2880$$

so condition (b) does not. Therefore admissible maps are not the same as equivariant maps for \mathcal{G}_{45} .

Remark 5.1. It can easily be shown that the linear admissible maps for \mathcal{G}_{mn} are the same as the linear equivariant maps, so the usual conditions for local bifurcation from a fully symmetric state are the same in both cases. However, the detailed nonlinear structure can be different, affecting the bifurcations: see Section 7.

The same calculation and a little extra effort proves:

Theorem 5.2. *The equivariant maps for $\mathbb{S}_m \times \mathbb{S}_n$ are the same as the admissible maps for \mathcal{G}_{mn} if and only if $(m, n) = (1, n), (2, 2), (2, 3), (3, 2)$.*

Proof. The vertex group of any node has order $v = (m-1)!(n-1)![(m-1)(n-1)]!$. This must be less than or equal to $|\mathbb{S}_m \times \mathbb{S}_n| = g = m!n!$. It is easy to show that this is the case if and only if $m = 1$, and n is arbitrary, or $(m, n) = (2, 2), (2, 3), (2, 4), (3, 2), (4, 2)$. We rule out $(2, 4)$ and $(4, 2)$ by considering the vertex group structure, not just its order.

If $m = 1$ then $v = (n-1)!$ and we must embed \mathbb{S}_{m-1} in \mathbb{S}_m , which is possible.

If $m = 2, n = 2$ we must embed $\mathbb{S}_1 \times \mathbb{S}_1 \times \mathbb{S}_1$ in $\mathbb{S}_2 \times \mathbb{S}_2$, which is possible.

If $m = 2, n = 3$ or the other way round we must embed $\mathbb{S}_1 \times \mathbb{S}_2 \times \mathbb{S}_2$ in $\mathbb{S}_2 \times \mathbb{S}_2$, which is possible.

If $m = 2, n = 4$ or the other way round we must embed $\mathbb{S}_3 \times \mathbb{S}_3$ in $\mathbb{S}_2 \times \mathbb{S}_4$. This is *not* possible. In $\mathbb{S}_3 \times \mathbb{S}_3$ there exist two non-conjugate order-3 elements, but in $\mathbb{S}_2 \times \mathbb{S}_4$ all order-3 elements are conjugate.

It remains to show that in the cases listed, all equivariants are admissible. This is trivial for $m = 1$ since it holds for an \mathbb{S}_n group network. For $(2, 2)$ the vertex groups are trivial. For $(2, 3)$, hence also $(3, 2)$, the vertex groups are $\mathbb{Z}_2 \times \mathbb{Z}_2$ with each factor acting independently on two arrows of a given type (solid, gray). These elements extend to automorphisms. The networks are all-to-all connected, so conditions (a) and (b) hold, which completes the proof. \square

This theorem suggests that there is scope for exotic colorings of opinion networks to exist. We confirm this by giving two examples of such colorings.

Example 5.3. In this example $m = 3, n = 6$ or $m = 6, n = 3$.

The 3×6 array in Figure 3 can be interpreted as an opinion network with 3 agents and 6 options — or, alternatively, 6 agents and 3 options. The trained Wilson network includes arrow of types (a), (b), (c) above, and we have seen that it is balanced for each type separately. The opinion network has a fourth type of arrow (d). By Lemma 3.4, the same coloring is also balanced for type (d) arrows, so it is balanced for the opinion network. This can also be checked directly by counting all input nodes of a given color.

Example 5.4. In the second example $m = 5, n = 5$.

The 5×5 network of Figure 4 can be interpreted as an opinion network, and again gives an exotic coloring.

It seems highly likely that similar constructions provide exotic patterns (both for trained Wilson networks and opinion networks) where $(m, n) = (k, 2k)$ for $k \geq 4$ and $(m, n) = (k, k)$ for $k \geq 6$. We have not investigated this question.

6 Wilson and Rivalry Networks

Recall that an untrained Wilson network \mathcal{W} consists of n disjoint columns, as in Figure 2. Each column is an all-to-all connected network (each pair of distinct nodes is connected in each direction by an arrow) in which all arrows are equivalent and inhibitory. Arrows in distinct columns are equivalent, and each column contains the same number m of

nodes. The nodes form an $m \times n$ array, and we label nodes by pairs (i, j) where $1 \leq i \leq m, 1 \leq j \leq n$.

Lemma 6.1. *The automorphism group of \mathcal{W} is the wreath product*

$$\Gamma = \mathbb{S}_m \wr \mathbb{S}_n$$

Proof. The assertion is a formal statement that automorphisms can permute the nodes in each column, independently, and also permute columns. \square

6.1 Colorings of Untrained Wilson Networks

We will prove that Wilson networks trained on 0, 1, or 2 patterns do not have exotic colorings. To do so, we require the following definition:

Definition 6.2. A partition of nodes is *color-disjoint* if nodes of the same color belong to the same part. That is, the colors refine the partition.

We also need the following proposition, which has some interest in its own right:

Proposition 6.3. *Let \mathcal{W} be an untrained Wilson network. Every balanced coloring of \mathcal{W} is the orbit coloring for an isotropy subgroup of Γ .*

Proof. All nodes of \mathcal{W} are input equivalent. Consider a coloring and let its isotropy subgroup be Σ . We claim that the coloring is given by the fixed-point set of Σ ; that is, colors are determined by the Σ -orbits.

If two columns contain a node with the same color, balance implies that every color occurs in each column with the same multiplicity. Using permutations of the columns, we can arrange all columns that share a color so that they are next to each other. This defines a partition of the set of columns. Call its parts ‘blocks’.

Within any given block, we can permute the nodes in those columns in any manner using Γ . Since colors occur with equal multiplicities, we can use such permutations to arrange the colors in rectangles, as in Figure 5. Call this the *standard form* of the coloring. It lies in the Γ -orbit of the original coloring because the permutations concerned lie in Γ . Their effect produces a coloring whose isotropy subgroup Σ' is conjugate to Σ , so without loss of generality we can consider a coloring in standard form.

We claim that the orbit coloring of Σ' is the standard coloring. By definition the standard coloring is fixed by Σ' . We must show that no finer coloring is fixed by Σ' . Since different blocks of columns are color-disjoint, it is enough to consider one block. Within that block, the rectangles are color-disjoint, so it is enough to consider a single rectangle. This rectangle is a Wilson network in its own right. Since all nodes have the same color, this is the orbit coloring for a subgroup of Σ isomorphic to $\mathbb{S}_q \wr \mathbb{S}_p$, where the rectangle has p rows and q columns. \square

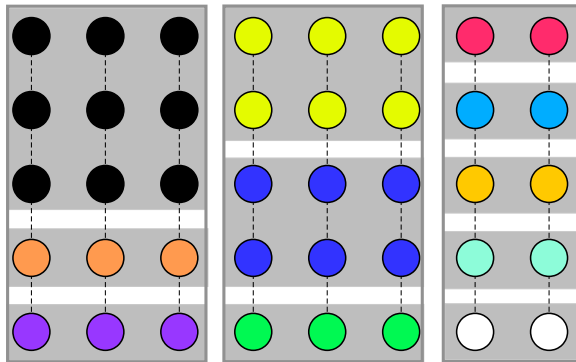


Figure 5: Partitioning an untrained Wilson network by a balanced coloring. Dotted lines indicate inhibitory connections within columns. Connections along each line are all-to-all, but for clarity they are shown only for adjacent nodes.

6.2 Training with Patterns

Define

$$M = \{1, \dots, m\} \quad N = \{1, \dots, n\}$$

so that nodes are labelled by $M \times N$. Here M parametrizes the rows and N the columns. A *pattern* is a function

$$f : N \rightarrow M \times N$$

such that for all $n \in N$ we have $f(n) = (g(n), n)$ for some $g(n) \in M$. Then g is a *section* of $M \times N$. We define \mathcal{C}^f to be the set of nodes of the form $(f(n), n)$ for $n \in N$.

We represent the learning of pattern f by \mathcal{W} as the introduction of new excitatory arrows, leading to a network \mathcal{W}^f . The new arrows are all identical, and one arrow connects each ordered pair of distinct nodes in $\mathcal{C}^f \times \mathcal{C}^f$. Learning a set of patterns $F = \{f_i\}$ is represented by adding one set of such arrows for each $f_i \in F$. The resulting network, denoted by \mathcal{W}^F , is a *trained Wilson network* or *rivalry network*.

Remark 6.4. This notion of learning implies that when two (or more) learned patterns have some nodes in common, those nodes receive two (or more) new arrows, not one.

In Wilson network models of visual illusions, learned patterns are replaced by patterns representing pre-learned geometric consistency conditions [40].

We assume that all of these excitatory arrows are identical for different f_i . It is easy to see that if f is a single pattern then every balanced coloring of \mathcal{W}^f is an orbit coloring. We prove the same is true for 2-colorings. (The method easily specializes to a single coloring.) First, we set up some useful observations.

Suppose that $F = \{f_1, f_2\}$ consists of two distinct patterns. Define the *input-type* of a node c to be the set of all nodes d such that $I(d)$ is input-isomorphic to $I(c)$. By [41, Section 6], any balanced coloring refines input-type. The network \mathcal{W}^F has precisely three distinct input-types:

Type A: Nodes that do not appear in a learned pattern. These have no excitatory connections and $m - 1$ inhibitory ones.

Type *B*: Nodes that appear in a single learned pattern: these have $n - 1$ excitatory connections and $m - 1$ inhibitory ones.

Type *C*: Nodes that appear in both learned patterns: these have $2n - 2$ excitatory connections and $m - 1$ inhibitory ones.

We also use A, B, C for the corresponding sets of nodes, Figure 6.

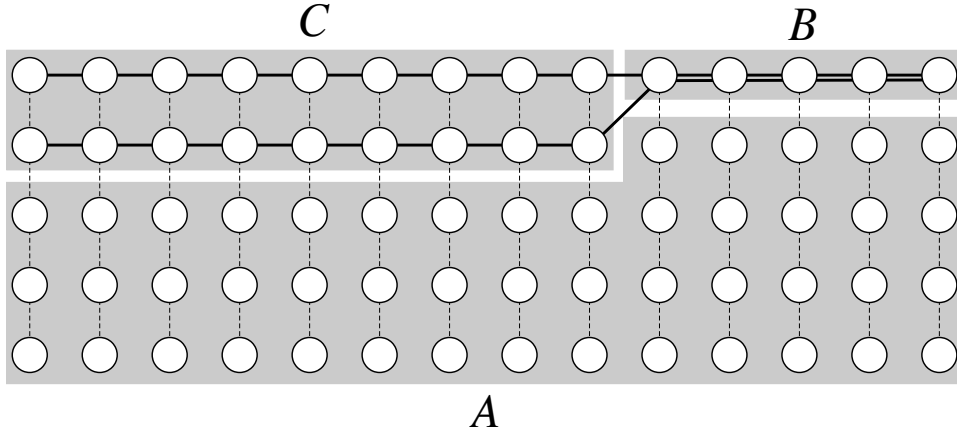


Figure 6: Partitioning a Wilson network with two learned patterns. Solid lines indicate learned excitatory connections, dotted lines indicate inhibitory connections within columns. Connections along each line are all-to-all, but for clarity these are shown only for adjacent nodes in each learned pattern.

Since a balanced coloring refines input equivalence, the partition $\{A, B, C\}$ is color-disjoint. These three types determine the group $\text{aut}(\mathcal{W}^F)$. It is a subgroup of $\text{aut}(\mathcal{W})$ (delete excitatory connections). It is generated by:

- (1) Permutations of the nodes in any given column that fix all nodes in B, C . These permute the nodes of type A in the column.
- (2) The permutation κ that fixes every node of type B and swaps the two nodes of type C in all columns that contain such nodes.
- (3) All permutations of those columns that contain nodes of type B .
- (4) All permutations of those columns that contain nodes of type C .

These permutations generate the subgroup

$$\Omega = \mathbb{Z}_2^\kappa \times (\mathbb{S}_{m-2} \wr \mathbb{S}_k) \times (\mathbb{S}_{m-1} \wr \mathbb{S}_{n-k}) \subseteq \mathbb{S}_m \times \mathbb{S}_n \quad (1)$$

Theorem 6.5. *Suppose that F consists of one or two distinct patterns. Then every balanced coloring of \mathcal{W}^F is a orbit coloring.*

Proof. We give the proof for two patterns; then we specialize to get the proof for one pattern. So let $F = \{f_1, f_2\}$ where $f_1 \neq f_2$.

We can use permutations within each column to arrange for nodes in learned patterns to appear as the top node, or top two nodes, of each column. Moreover, nodes in the same f_j appear in the same row when the patterns are distinct in that column. Permutations between columns can position all the nodes that belong to two patterns first (reading along rows from left to right), followed by those that belong to only one, as in Figure 6.

The network \mathcal{W}^F has precisely three distinct input-types A, B, C , defined above. Since a balanced coloring refines input equivalence, the partition $\{A, B, C\}$ is color-disjoint.

Suppose that the top two rows of region C have a color in common. The all-to-all excitatory connections, plus balance, then imply that every color appearing in the top row must also appear in the bottom row, with the same multiplicity.

There are thus two cases:

Case 1: Every color appearing in the top row must also appear in the bottom row, with the same multiplicity.

Case 2: The two rows of region C are color-disjoint.

First, we deal with Case 1.

We refine the partition $\{A, B, C\}$ in two further stages. First we split regions C into two parts C_1, C_2 as follows. If a node in row 1 has an inhibitory connection to a node with the same color in row 2, (necessarily in the same column), place those nodes in set C_1 . Otherwise place them in C_2 .

We claim that each vertical connection in C_2 links the same two (distinct) colors. Suppose a node in row 1 has color α and is connected to color β in row 2. Balance implies that every node of color α in either row must be paired vertically with color β in the other row. Moreover, both rows contain the same number of nodes with any given color, so colors α and β occur with the same multiplicity in row 1 and in row 2. (In particular, C_2 meets an even number of columns.)

Clearly C_1 and C_2 are color-disjoint, by balance. A color anywhere in C_1 cannot connect vertically both to itself, and to something different. (Bear in mind that regions C and A are color-disjoint, so the discrepancy cannot be repaired by coloring another node in the same column.) We now split region A into A_1, A_2, A_3 , according to whether the top node of the column lies in C_1, C_2 , or B . Balance clearly implies that all six regions $A_1, A_2, A_3, B, C_1, C_2$ are color-disjoint. See Figure 7.

Finally, we partition regions C_1 and B according to the color of the top node. Region C_2 is similarly partitioned using the colors of the vertical pairs in the top two rows. (Only one such subset is drawn but there could be many.) Without loss of generality we can use elements of Ω , defined in (1), to group nodes of a given color (or color pair) into blocks of adjacent nodes, Figure 8.

As in the proof of Proposition 6.3, we can use elements of Ω to arrange colors in the blocks of A_j into rectangles, each rectangle containing a single color. Recall that κ flips the two learned patterns (acting trivially on B). Define a permutation ρ of the columns, of order 2, which acts trivially on B, C_1 and transposes pairs of adjacent columns in C_2

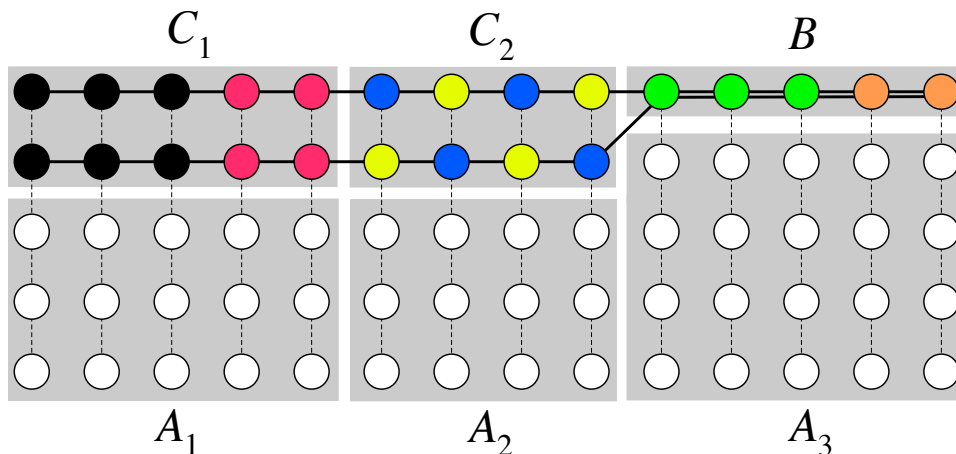


Figure 7: Refining the partition of the trained Wilson network by splitting regions A, C .

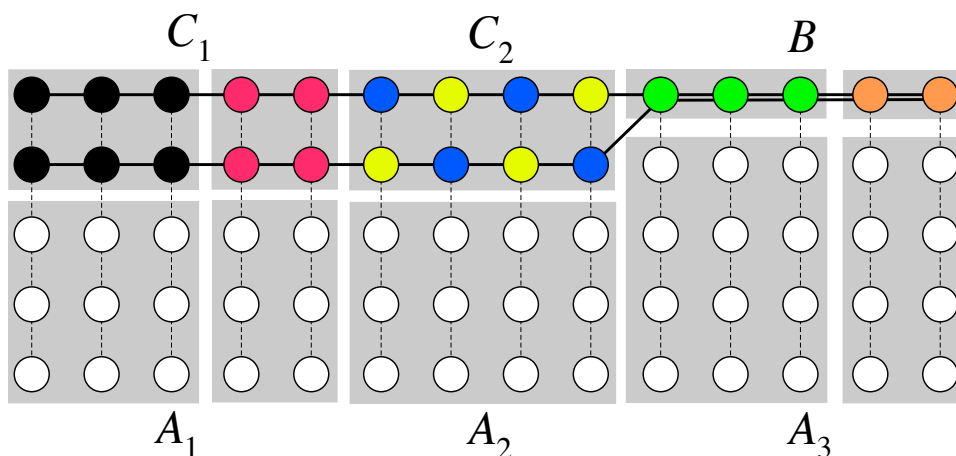


Figure 8: Refining the partition of the trained Wilson network even further by splitting regions according to colors appearing in the learned patterns.

with matching colors in their top nodes. Then $\kappa\rho$ fixes all the colors of nodes in $B \cup C$. Further permutations of the columns force equalities of colors along the top row.

We now construct, for any rectangle R in any region, a subgroup $\Sigma_R \subseteq \Sigma$ whose fixed-point set determines the coloring in that rectangle. The subgroup generated by all such permutations, together with $\kappa\rho$ and any permutations of columns already defined, has the same fixed-point set as Σ because Σ is the isotropy group of the coloring. The construction of Σ_R is the same as that in the proof of Proposition 6.3, giving a group $\mathbb{S}_q \wr \mathbb{S}_p$ where the rectangle has p rows and q columns. This completes Case 1.

Case 2 is similar, but now the two rows of C are color-disjoint, so $\kappa\rho$ is not required. This completes the proof for two learned patterns.

When there is only one learned pattern, the same proof applies taking C to be the empty set. Now every arrow in B occurs twice, but this is effectively the same as a single arrow of a new type. \square

The network of Figure 3 can be viewed as a trained Wilson network with three

(disjoint) learned patterns. Thus the analog of Theorem 6.5 is not valid for Wilson networks with three learned patterns. Similarly, The network of Figure 4 can be viewed as a trained Wilson network with five (disjoint) learned patterns.

7 Bifurcations to Exotic Patterns

We comment briefly on the implications of Figure 4 for bifurcations. The corresponding analysis for Figure 3 is less straightforward when colors are amalgamated to apply the Equivariant Branching Lemma, and we have not carried it out.

Associated with any balanced coloring K of a network \mathcal{G} is a *quotient network* \mathcal{G}_K with one node for each color, and input arrows copied from the original network according to the colors of head and tail nodes. It is shown in [20, 41] that with canonical identifications of state spaces, the restriction of an admissible map for \mathcal{G} to the synchrony subspace of K is admissible for \mathcal{G}_K , and all admissible maps for \mathcal{G}_K can be obtained in this manner.

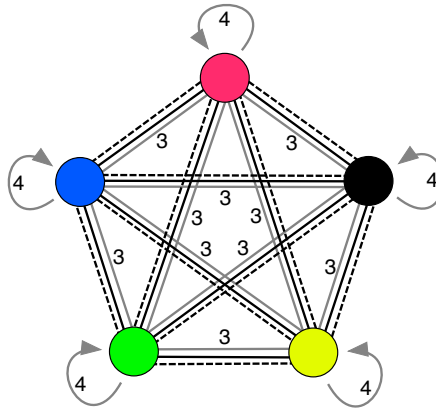


Figure 9: The quotient network for Figure 4. Lines without arrows are bidirectional. Numbers beside gray arrows indicate multiplicities.

The quotient network for the coloring in Figure 4 is shown in Figure 9. It has five nodes and \mathbb{S}_5 symmetry. It is easy to see that *any* coloring of this quotient network is balanced; indeed, it is an orbit coloring for the subgroup of \mathbb{S}_5 that preserves the colors of nodes. Moreover, balanced colorings lift from quotient networks to the original network, and remain balanced. However, the lift need not be an orbit coloring on the full network, as we now demonstrate.

We can apply the Equivariant Branching Lemma to this quotient, and then lift the resulting pattern to \mathcal{G}_{55} , to prove the generic existence of branches with (for instance) two colors, obtained by amalgamating colors in Figure 4 in any manner. The question is whether any of these amalgamated colorings is exotic for \mathcal{G}_{55} . Some are not, but a plausible candidate is Figure 10 (left), obtained by coloring black and yellow the same, and red, green, and blue the same. We claim that this pattern is indeed exotic in \mathcal{G}_{55} . The proof uses Proposition 3.3.

Calculations with Mathematica show that the isotropy subgroup $\Sigma \subseteq \mathbb{S}_5 \times \mathbb{S}_5$ of Figure 10 (left) is isomorphic to a dihedral group \mathbb{D}_5 . Since this acts on 25 nodes, and

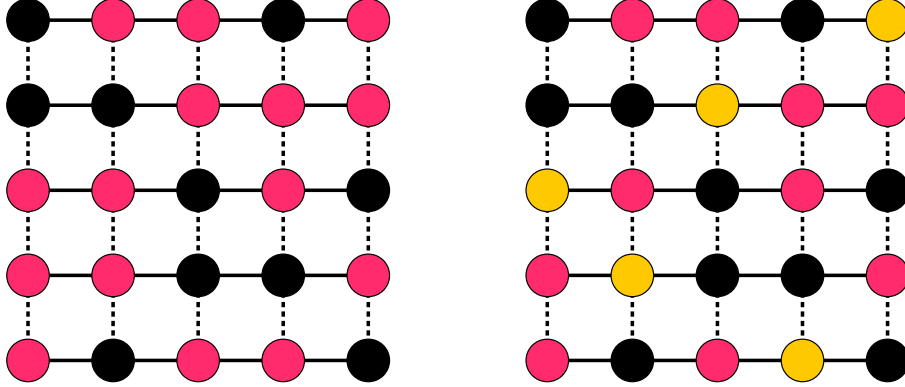


Figure 10: *Left*: This balanced 2-coloring is not an orbit coloring for $\mathbb{S}_5 \times \mathbb{S}_5$. *Right*: The fixed-point subspace of the isotropy subgroup of the 2-color pattern is a 3-color pattern.

its orbits have size at most 10, there must be at least 3 orbits, so its fixed-point subspace must have dimension at least 3. Therefore Figure 10 is not an orbit coloring for $\mathbb{S}_5 \times \mathbb{S}_5$.

In more detail: the group Σ is generated by the pairs of permutations (in cycle notation)

$$g = ((13245), (13245)) \quad h = ((1)(24)(35), (14)(23)(5))$$

which satisfy the relations

$$g^5 = h^2 = 1, \quad hgh = g^{-1}$$

for \mathbb{D}_5 . It is a twisted \mathbb{D}_5 subgroup of \mathbb{S}_5 ; that is, it consists of elements $(\gamma, \theta(\gamma))$ where $\gamma \in \mathbb{D}_5 \subseteq \mathbb{S}_5 \times \mathbf{1}$ and $\theta : \mathbb{D}_5 \rightarrow \mathbb{D}_5$ is an isomorphism. Up to conjugacy we can make θ the identity on \mathbb{Z}_5 ; it then maps an order-2 element to a different order-2 element.

The fixed-point subspace of Σ comprises the patterns in Figure 10 (right). There are two orbits of size 10 (black, red) and one of size 5 (orange). By Lemma 3.4, this 2-coloring is not an orbit coloring. (The orange nodes do *not* correspond to a specific color in Figure 4 (left): the reason is that this 5-coloring is not an orbit coloring.)

The quotient network for the 3-coloring of Figure 10 (right), which we do not draw, has an obvious \mathbb{Z}_2 symmetry that swaps red and black but fixes orange. It has an orbit coloring that merges red and black. It also has a balanced coloring that merges red and orange, which is not a \mathbb{Z}_2 orbit coloring, and this lifts to Figure 10 (right).

7.1 Stability

As well as existence of particular states, it is also important to study their stability. This is a more delicate issue. In particular, whenever the critical eigenspace supports a nontrivial equivariant quadratic, all axial bifurcating branches of equilibria are *unstable* near the bifurcation point; see [19, Chapter XIII Theorem 4.4]. When the symmetry group is \mathbb{S}_n in its standard permutation representation, and we are considering a symmetry-breaking bifurcation, such a quadratic equivariant exists for all $n \geq 3$. This problem also arises for $\mathbb{S}_m \times \mathbb{S}_n$. It is discussed in the evolutionary models of [6, 15, 37], for \mathbb{S}_n , and in the decision models of [12] for $\mathbb{S}_m \times \mathbb{S}_n$. In both cases the remedy is to include suitable cubic equivariant terms to ‘compactly’ the bifurcation. This allows an unstable transcritical

branch to turn around at a saddle-node (fold) point and regain stability. This creates a jump bifurcation. (If $n = 2k$ there is an exception: the isotropy subgroup $\mathbb{S}_k \times \mathbb{S}_k$ gives a pitchfork bifurcation.)

The same issue arises when considering the stability of the pattern in Figure 10 (left), because the symmetry group of the quotient network is \mathbb{S}_5 , and on the relevant synchrony subspace the pattern is given by an axial subgroup $\mathbb{S}_2 \times \mathbb{S}_3$. The same remedy also applies: include suitable cubic equivariants so that the branch turns round. It can then regain stability within the synchrony subspace. This still leaves open whether it is also stable transverse to the synchrony subspace, that is, to perturbations that break the synchrony of the balanced 5-coloring. We have not yet investigated this question, but the problem is likely to be complicated.

Numerical simulations in [12] suggest that states arising from axial subgroups of $\mathbb{S}_5 \times \mathbb{S}_5$ can be stabilized in this manner in the whole of state space \mathbb{R}^{25} . However, this particular state has not yet been explored numerically.

8 Conclusions

We have studied the formation of synchrony patterns in networks \mathcal{G}_{mn} whose nodes form $m \times n$ arrays, and whose connections imply $\mathbb{S}_m \times \mathbb{S}_n$ symmetry. Symmetry methods — namely, the Equivariant Branching Lemma and the Equivariant Hopf Theorem — prove the generic existence of bifurcating branches that break symmetry to, respectively, axial subgroups and \mathbb{C} -axial subgroups.

Network structure is stronger than equivariance, and it can create exotic colorings, not predicted by symmetry considerations. Such colorings exist in particular when $(m, n) = (3, 6)$ and $(5, 5)$.

Applying the Equivariant Branching Lemma to a quotient network of \mathcal{G}_{55} , we have proved the existence of an exotic 2-coloring of \mathcal{G}_{55} itself. This pattern is unstable near bifurcation. It can regain stability in the quotient network, but may still be unstable to perturbations that break the synchrony pattern defining that quotient.

Networks \mathcal{G}_{mn} have been used to model decision making, and related networks to which the same results apply occur in models of binocular rivalry and visual illusions. The occurrence of exotic synchrony patterns predicts states of such models that have not been derived using equivariant methods, and whose description is not given by isotropy subgroups.

We have also shown that in rivalry models, networks trained on one or two images do not have exotic colorings, so all synchrony patterns (hence also all phase patterns) can be characterized by isotropy subgroups of the symmetry group.

References

- [1] F. Antoneli and I. Stewart. Symmetry and synchrony in coupled cell networks 1: fixed-point spaces, *Internat. J. Bif. Chaos* **16** (2006) 559-577.

- [2] F. Antoneli and I. Stewart. Symmetry and synchrony in coupled cell networks 2: group networks, *Internat. J. Bif. Chaos* **17** (2007) 935-951.
- [3] F. Antoneli and I. Stewart. Symmetry and synchrony in coupled cell networks 3: exotic patterns, *Internat. J. Bif. Chaos* **18** (2008) 363-373.
- [4] A. Bizyaeva, A. Franci, and N.E. Leonard. A general model of opinion dynamics with tunable sensitivity, arXiv:2009.04332 [math.OC] (2020).
- [5] G. Cicogna. Symmetry breakdown from bifurcations, *Lettere al Nuovo Cimento* **31** (1981) 600–602.
- [6] J. Cohen and I. Stewart. Polymorphism viewed as phenotypic symmetry-breaking, in *Nonlinear Phenomena in Biological and Physical Sciences* (eds. S.K. Malik, M.K. Chandrasekharan, and N. Pradhan), Indian National Science Academy, New Delhi 2000, 1–63.
- [7] R. Curtu. Singular Hopf bifurcations and mixed-mode oscillations in a two-cell inhibitory neural network, *Physica D* **239** (2010) 504–514.
- [8] R. Curtu, A. Shpiro, N. Rubin, and J. Rinzel. Mechanisms for frequency control in neuronal competition models, *SIAM J. Appl. Dynam. Sys.* **7** (2008) 609–649.
- [9] C. Diekman, M. Golubitsky, T. McMillen, and Y. Wang. Reduction and dynamics of a generalized rivalry network with two learned patterns, *SIAM J. Appl. Dynam. Sys.* **11** (4) (2012) 1270–1309.
- [10] C. Diekman, M. Golubitsky, and Y. Wang. Derived patterns in binocular rivalry networks, *J. Math. Neuro.* **3** (6) (2013); doi10.1186/2190-8567-3-6.
- [11] C. Diekman and M. Golubitsky. Network symmetry and binocular rivalry experiments, *J. Math. Neuro.* **4** (2014); DOI 10.1186/2190-8567-4-12.
- [12] A. Franci, M. Golubitsky, A. Bizyaeva, and N.E. Leonard. A model-independent theory of consensus and dissensus decision making, preprint 2020.
- [13] M. Golubitsky, M. Nicol, and I. Stewart. Some curious phenomena in coupled cell networks, *J. Nonlinear Sci.* **14** (2004) 207–236.
- [14] M. Golubitsky, D. Romano and Y. Wang. Network periodic solutions: full oscillation and rigid synchrony, *Nonlinearity* **23** (2010) 3227–3243.
- [15] M. Golubitsky and I. Stewart. *The Symmetry Perspective*, Progress in Mathematics **200**, Birkhäuser, Basel 2002.
- [16] M. Golubitsky and I. Stewart. Nonlinear dynamics of networks: the groupoid formalism, *Bull. Amer. Math. Soc.* **43** (2006) 305–364.
- [17] M. Golubitsky and I. Stewart. Recent advances in symmetric and network dynamics, *Chaos* **25** (2015) 097612; DOI: 10.1063/1.4918595.

- [18] M. Golubitsky and I. Stewart. Rigid patterns of synchrony for equilibria and periodic cycles in network dynamics, *Chaos* **26** (2016) 094803; DOI: 10.1063/1.4953664.
- [19] M. Golubitsky, I. Stewart, and D.G. Schaeffer. *Singularities and Groups in Bifurcation Theory II*, Applied Mathematics Series **69**, Springer, New York 1988.
- [20] M. Golubitsky, I. Stewart, and A. Török. Patterns of synchrony in coupled cell networks with multiple arrows, *SIAM J. Appl. Dynam. Sys.* **4** (2005) 78–100.
- [21] M. Golubitsky, Y. Zhao, Y. Wang, and Z. Lu. Symmetry of generalized rivalry network models determines patterns of interocular grouping in four-location binocular rivalry, *J. Neurophysiol.* **122** (2019) 1989–1999.
- [22] G.J. Kalarickal and J.A. Marshall. Neural model of temporal and stochastic properties of binocular rivalry, *Neurocomputing* **32** (2000) 843–853.
- [23] I. Kovács, T.V. Papathomas, M. Yang, and A. Fehér: When the brain changes its mind: interocular grouping during binocular rivalry, *Proc. Nat. Acad. Sci.* **93** (1996) 15508–15511.
- [24] C.R Laing and C.C. Chow. A spiking neuron model for binocular rivalry, *J. Comput. Neurosci.* **12** (2002) 39–53.
- [25] S.R. Lehky. An astable multivibrator model of binocular rivalry, *Perception* **17** (1988) 215–228.
- [26] K. Matsuoka. The dynamic model of binocular rivalry, *Biol. Cybern.* **49** (1984) 201–208.
- [27] T.J. Mueller. A physiological model of binocular rivalry, *Vis. Neurosci.* **4** (1990) 63–73.
- [28] L.A. Necker. Observations on some remarkable optical phænomena seen in Switzerland; and on an optical phænomenon which occurs on viewing a figure of a crystal or geometrical solid, *London and Edinburgh Philosophical Magazine and Journal of Science* **1** (1832) 329–337.
- [29] A.J. Noest, R. van Ee, M.M. Nijs, and R.J.A. van Wezel. Percept-choice sequences driven by interrupted ambiguous stimuli: a low-level neural model, *J. Vis.* **7** (2007) 10; doi: 10.1167/7.8.10.
- [30] L.M. Pecora, F. Sorrentino, A.M. Hagerstrom, T.E. Murphy, and R. Roy. Symmetries, cluster synchronization, and isolated desynchronization in complex networks, *Nature Communications* **5** (2013); doi: 10.1038/ncomms5079.
- [31] G. della Porta. *De Refractione. Optices Parte. Libri Novem*, Salviani, Naples 1593.
- [32] J. Seely and C.C. Chow. The role of mutual inhibition in binocular rivalry, *J. Neurophysiol.* **106** (2011) 2136–2150.

- [33] S.K. Shevell, R. St Clair, and S.W. Hong. Misbinding of color to form in afterimages, *Vis. Neurosci.* **25** (2008) 355-360.
- [34] I. Stewart. The lattice of balanced equivalence relations of a coupled cell network, *Math. Proc. Camb. Phil. Soc.* **143** (2007) 165–183.
- [35] I. Stewart. Exotic patterns of synchrony in planar lattice networks, *Internat. J. Bif. Chaos* **29** (2019) 1939993; doi: 10.1142/S0218127419300039.
- [36] I. Stewart. Overdetermined constraints and rigid synchrony patterns for network equilibria, *Portugaliae Mathematica* **77** (2020) 163–196.
- [37] I. Stewart, T. Elmhirst, and J. Cohen. Symmetry-breaking as an origin of species, in *Bifurcations, Symmetry, and Patterns* (eds. J. Buescu, S. Castro, A.P.S. Dias, and I. Labouriau), Birkhäuser, Basel 2003, 3–54.
- [38] I. Stewart and D. Gökaydin. Symmetries of quotient networks for doubly periodic patterns on the square lattice, *Internat. J. Bif. Chaos* **29** (2019) 1930026; doi: 10.1142/S021812741930026X.
- [39] I. Stewart and D. Gökaydin. Symmetries of quotient networks for doubly periodic patterns on the hexagonal lattice, *Internat. J. Bif. Chaos* **30** (2020) 2030004; doi: 10.1142/S0218127420300049.
- [40] I. Stewart and M. Golubitsky. Symmetric networks with geometric constraints as models of visual illusions, *Symmetry* **11** (2019) 799; doi: 10.3390/sym11060799.
- [41] I. Stewart, M. Golubitsky, and M. Pivato. Symmetry groupoids and patterns of synchrony in coupled cell networks, *SIAM J. Appl. Dynam. Sys.* **2** (2003) 609–646.
- [42] S. Suzuki and M. Grabowecky. Evidence for perceptual ‘trapping’ and adaptation in multistable binocular rivalry, *Neuron* **36** (2002) 143–157.
- [43] F. Tong, M. Meng, and R. Blake. Neural bases of binocular rivalry, *Trends in Cognitive Sciences* **10** (2006) 502–511.
- [44] Wikipedia. Latin square, https://en.wikipedia.org/wiki/Latin_square.
- [45] H. Wilson. Computational evidence for a rivalry hierarchy in vision, *Proc. Nat. Acad. Sci.* **100** (2003) 14499–14503.
- [46] H. Wilson. Minimal physiological conditions for binocular rivalry and rivalry memory, *Vision Research* **47** (2007) 2741–2750.
- [47] H.R. Wilson. Requirements for conscious visual processing, in: *Cortical mechanisms of vision* (eds. M. Jenkin and L. Harris), Cambridge University Press, Cambridge 2009, 399–417.